JOURNAL OF MATERIALS SCIENCE 9 (1974) 576–582

High temperature plasticity of lithium zinc silicate glass-ceramics

Part 1 *Constant strain-rate tests*

R. LYALL*, K. H. G. ASHBEE
H. H. Wills Physics Laboratory, University of Bristol, Bristol, UK

Constant strain-rate tensile and compressive tests have been carried out on specimens of a glass-ceramic derived from the SiO_2-Li_2O-ZnO system. With increasing temperature, the tensile strength decreases from its room temperature value to a minimum at approximately 500°C and then increases to a peak strength of nearly 2 kbar at about 650°C before falling to almost zero above 800°C. The ultimate strength at high temperatures is considerably greater in compression than in tension and, in compression, it is succeeded by plasticity at progressively smaller levels of stress. The apparent absence of microstructural change during plastic deformation suggests that the hot glass-ceramic behaves as a rigid solid/viscous fluid mixture, the properties of which are briefly discussed.

1. Introduction

The devitrification of glasses can be stimulated by certain physical and chemical agents and controlled by suitable heat-treatments to yield fine grained ceramic materials which, if the distribution of internal stress generated by the differential thermal contraction of the constituent phases is such that fracture is inhibited, are called glass-ceramics. Since the volume fraction of crystalline material is always significantly less than 100%, it is necessary to analyse the properties of a glass-ceramic in terms of the behaviour expected for a mixture of crystalline and non-crystalline materials which, for high temperature properties, may mean in terms of a solid/liquid mixture.

Morrell and Ashbee [1] have reported detailed studies of the high temperature tensile and compressive creep properties of lithium zinc silicate glass-ceramics. For a given stress and temperature, these materials creep very much faster in tension than in compression. The stress exponents for steady state creep vary from 1 to 6 suggesting that the mechanisms of secondary creep that commonly occur in polycrystalline metals, for example, are not dominant. This is true for both signs of applied stress.

The plasticity of the same materials is further explored here by making high temperature constant strain-rate tests.

2. Materials and specimen preparation

The SiO_2-Li_2O-ZnO system was chosen for this investigation since the necessary refining temperatures are relatively low. The raw materials were general laboratory grades of precipitated silica, lithium carbonate, zinc oxide, hydrated zinc orthophosphate and potassium nitrate obtained from the British Drug Houses Ltd. Phosphorus pentoxide is a satisfactory nucleating agent [2] for this system and the presence of potassium oxide lowers the viscosity of the non-crystalline material so that shear stresses are easily relieved and thermal shock is prevented [3]. Preliminary melting and crystallization experiments showed that a satisfactory glass composition is SiO_2 71.4%, Li_2O 12.5%, ZnO 11.5%, P_2O_5 2.1% and K_2O 2.5% by weight respectively. 1 lb† batches were weighed, intimately mixed, ground, melted in platinum

---

*Now at Wilkinson Sword Laboratories, Stoke Poges, Bucks.
†1 lb = 0.4536 kg.

crucibles and quenched into water at room temperature. After drying, the quenched glass was thoroughly mixed in batches of several lb. and then refined in 30 ml platinum crucibles for 4 h at 1300°C.

To manufacture tensile specimens, rods 15 cm long × 0.95 cm diameter were cast into graphite moulds pre-heated to 450°C. The as-cast glass rods were divided into bundles of 15, packed horizontally in silica flour and heated at 10°C min^{-1} to 475°C. After a 1 h nucleation period, the temperature was raised at 2°C min^{-1} to 850°C and, after a further hour at this upper crystallization temperature, the rods were furnace cooled to room temperature. A gauge length 3 cm long × 0.6 cm diameter was ground into the middle section of each rod using a milling machine which incorporates a diamond impregnated wheel. The specimen ends were scored and bonded into water-cooled grips, Figure 1. During curing of the epoxy resin bonding medium, axial alignment was ensured by mounting each specimen/grips assembly in a specially designed jig. The tensometer used for testing these specimens is a hard beam, constant crosshead machine.

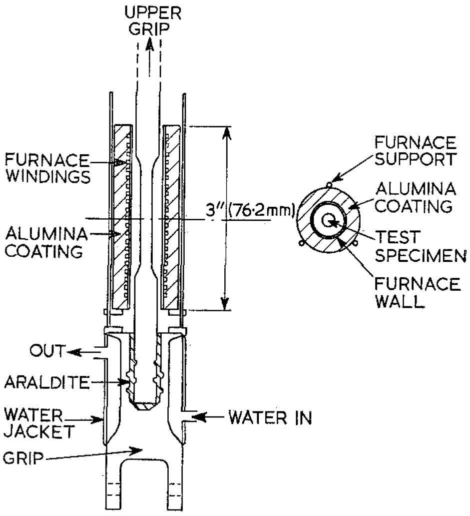

Figure 1 Specimen/grip and furnace assemblies.

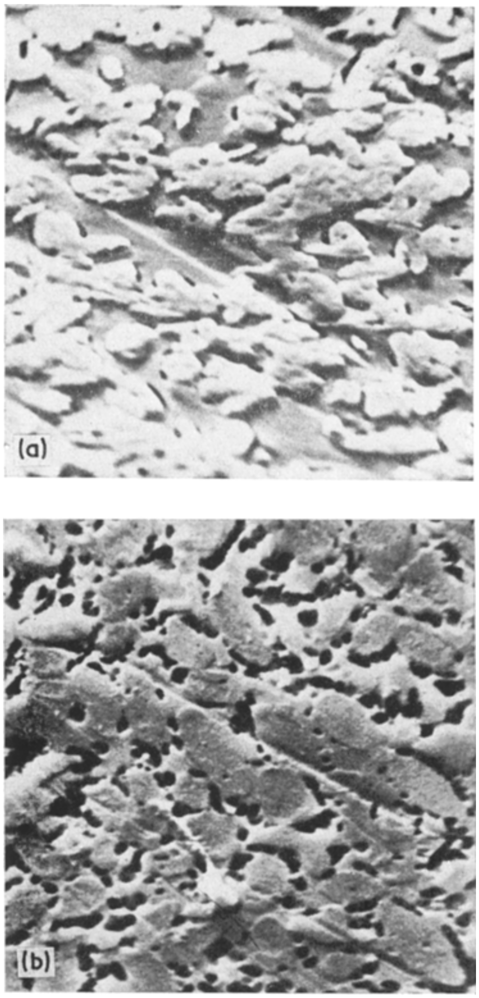

Figure 2 Scanning electron micrographs of lightly etched sections of (a) partially and (b) fully crystallized specimens (×6000).

Compression test specimens were prepared from the same glass by sucking melt into pre-heated graphite tubes of 0.25 cm internal bore. When solid, the lengths of glass were withdrawn and sawn into cylinders 0.5 cm long. These were crystallized according to the schedule described above and tested using a compression jig incorporated into the tensile machine.

3. As-crystallized structure

The crystallization process was investigated in specimens quickly cooled to room temperature after various times into the heat-treatment schedule. Microstructural observations were made using optical and scanning electron microscopy, and phases were identified by taking X-ray diffraction patterns from powdered samples.

Lithium disilicate was the first crystalline phase detected, grains of which appeared at

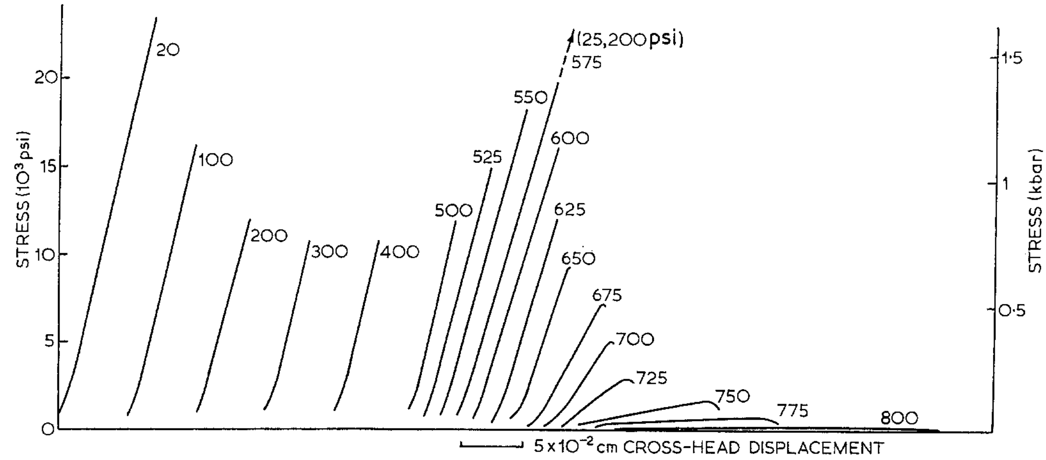

Figure 3 Nominal tensile stress versus crosshead displacement at various temperatures. Specimen gauge length 3 cm, nominal strain-rate 3 × 10^{-5} sec^{-1}. The numbers denote test temperatures in °C.

575°C (Fig. 2a) and continued to grow more or less as spherulites to diameters of up to 3 μm (Fig. 2b). The smaller crystals in Fig. 2b are a mixture of β-zinc silicate and lithium zinc silicate, many grains of which appear to grow from nucleation sites on lithium disilicate crystal surfaces. In fully heat-treated specimens, the proportion of crystalline material was estimated from line measurements to be about 80% by volume and assuming stoichiometric compositions for the crystalline phases, the composition of the residual glass is approximately SiO_2 88, K_2O 12 wt% respectively. However, the residual glass may also contain traces of Li_2O, ZnO and P_2O_5.

Where neighbouring grains impinge, grain growth appears to terminate either in the form of a grain-glass-grain interface or as a grain-grain boundary. Both forms appear in the partially and fully crystallized samples (Fig. 2a and b) and substantiate the ideas of Filipovich [4] who, from energy considerations, argues that grain-glass-grain boundaries will dominate except when the approaching grains are closely matched both chemically and atomically. In the present glass-ceramic, grain-glass-grain boundaries are in the majority, but the evidence for thin intergranular crystalline links suggests that the structure may be regarded as two interwoven continuous networks, one crystalline and the other non-crystalline.

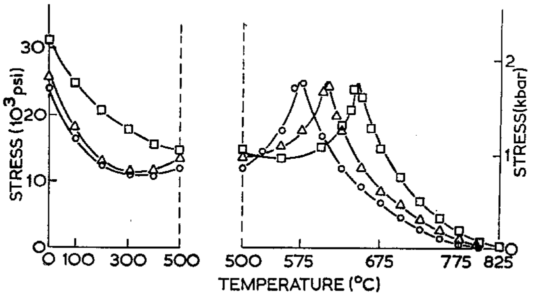

Figure 4 Nominal maximum tensile stress as a function of the temperature. Nominal strain-rates, ○, 3 × 10^{-5} sec^{-1}, △ 3 × 10^{-4} sec^{-1}, □ 3 × 10^{-3} sec^{-1}.

4. Constant extension rate tests

Examples of the nominal stress (instantaneous load divided by the original area of cross-section) versus crosshead displacement, measured at a nominal strain-rate (crosshead speed divided by the original gauge length) of 3 × 10^{-5} sec^{-1} and in the temperature range 20 to 825°C, are given in Fig. 3. Fig. 4 shows the dependence of maximum stress on both temperature and strain-rate. Below a certain temperature (625°C at 3 × 10^{-5} sec^{-1}) the maximum stress is the fracture stress and, at higher temperatures, it is slightly greater than the fracture stress.*

The general form of the strength-temperature-strain rate relationship, Fig. 4, demonstrates the effects of non-elastic processes on fracture. At temperatures below 450°C, the glass-ceramic behaves as a multi-phase brittle solid that is susceptible to static fatigue. At higher tem-

---

*The plasticity which evidently precedes failure at high temperatures is discussed in Part 2.

peratures, thermally activated mechanisms are dominant. Of particular interest is the temperature dependence of fracture stress at temperatures above that corresponding to the peak strength. If the microstructure consists of isolated crystalline masses within a continuous glassy matrix, the high temperature tensile strength must be determined by surface tension forces in the glass. However, the variations with temperature are too great to be due to surface tension alone and can be satisfactorily explained only if fracture is governed by failure of a continuous crystalline network.

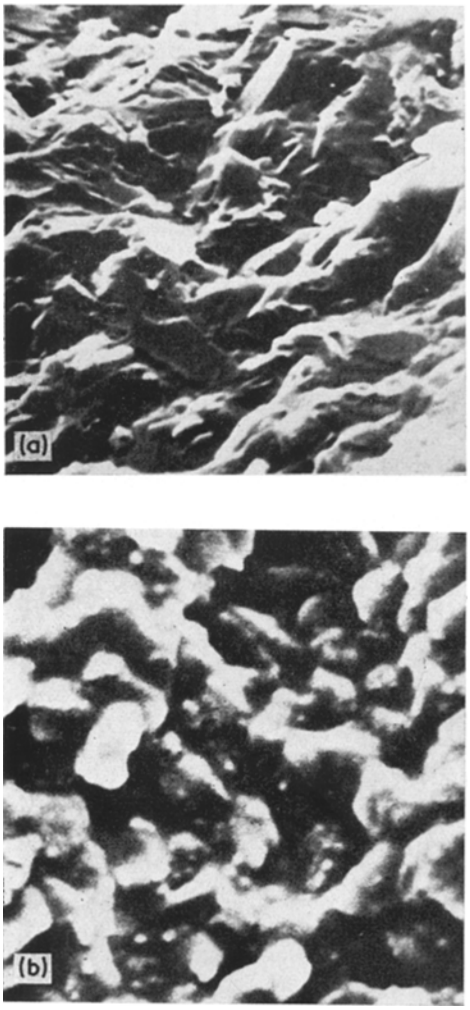

Figure 5 Scanning electron micrographs illustrating the nature of fracture surfaces obtained at (a) below 625° C (b) above 750° C. Notice the glass covered crystals in evidence at high temperatures (×6000).

The occurrence of a sharp peak in the strength versus temperature relationship is accompanied by a change in fracture mode from mixed intergranular and transgranular fracture at low temperatures to wholly intergranular failure at high temperatures. For a given strain-rate, intergranular fracture surfaces are first resolved at 25° C above the temperature corresponding to peak strength, compare Fig. 5 with Fig. 4. The temperature lag presumably arises because the appearance of a fracture surface is determined by the overall nature of crack propagation, whereas the fracture stress is more strongly dependent on crack initiation.

The fact that the fracture stress is sensitive to both temperature and strain-rate suggests that it may be determined by thermally activated processes. Assuming that a single thermally activated process is dominant at each temperature, the strain-rate can be written as

$$\dot{\epsilon} = Af(\sigma) \exp - \frac{H}{RT}$$

Thus, for a given stress

$$\ln\left(\frac{\dot{\epsilon}_1}{\dot{\epsilon}_2}\right) = \frac{H}{R}\left(\frac{T_1 - T_2}{T_1\, T_2}\right).$$

Applying this to the results shown in Fig. 4 reveals the existence of just two distinct activation energies, see Fig. 6. At low temperatures, the dominant process has an activation energy of

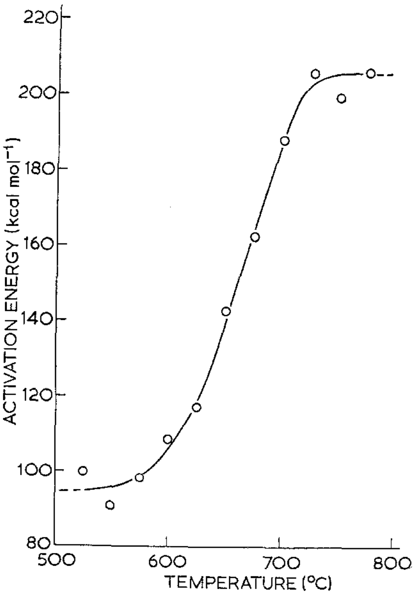

Figure 6 Relation between activation energy for maximum tensile stress and temperature.

95 kcal mol^{-1} and this is of the order expected for flow of a low activation energy glass [5, 6]. The process dominant at higher temperatures has an activation energy of 200 kcal mol^{-1}, which is a reasonable figure for plastic deformation in ceramic crystals.

5. Constant compression rate tests

Fig. 7 shows examples of the nominal compressive stress (instantaneous load divided by the original area of cross-section) versus crosshead displacement at temperatures in the plastic range, i.e. above 650° C. At stresses up to 30 to 50 times the tensile strength, the strains are of the order of elastic strains. Thereafter, large scale plastic deformation occurs; the stress slowly rises to a maximum value and then usually decreases with further compression until the specimen crumbles between the compression plattens, see Fig. 8. The maximum nominal compressive stress is temperature and strain-rate dependent, Fig. 9.

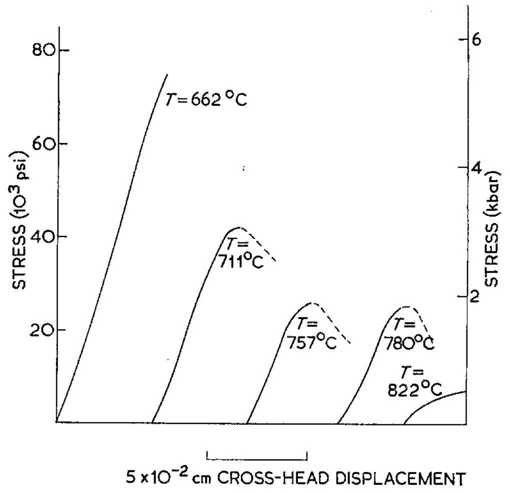

Figure 7 Nominal compressive stress versus crosshead displacement at various temperatures. Nominal strain-rate 3×10^{-3} sec^{-1}. The "work-softening" (broken lines) is not reproducible.

6. Discussion

Attempts to investigate the plasticity using the direct observation techniques of optical microscopy, scanning electron microscopy and electron probe X-ray microanalysis were not very successful. Except after very large compressive deformations, there were no resolvable changes

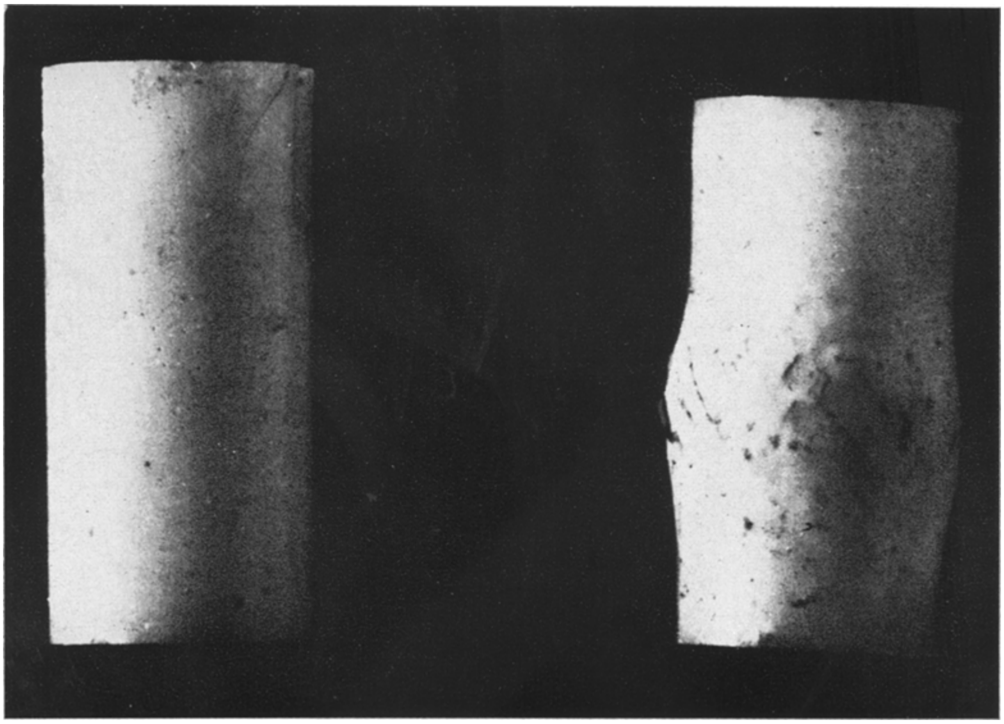

Figure 8 Compression specimen before and after compressing at 750°C. Nominal strain-rate 3×10^{-5} sec^{-1}.

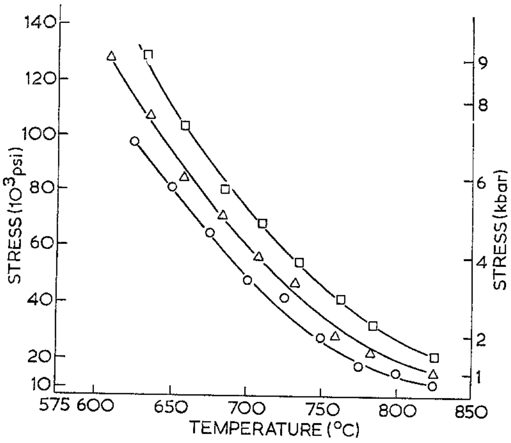

Figure 9 Nominal maximum compressive stress as a function of temperature. Nominal strain-rates, ○, 3×10^{-5} sec^{-1}, △, 3×10^{-4} sec^{-1}, □, 3×10^{-3} sec^{-1}.

in appearance of external surfaces or of polished and etched sections. Also, in a previous investigation [7], there was no evidence for deformation textures in the crystalline material of a glass-ceramic of similar composition to that used here. We are, therefore, led to conclude that there is little or no plastic deformation within the crystalline material and, hence, that the granular masses (spherulites) are displaced rigidly with respect to each other.

Assuming that the arrangement of spherulites is best packed to start with, shear must be accompanied by dilatancy, that is by an increase in the volume of the interstitial fluid, and the consequent decrease in fluid pressure is expected to enhance any frictional resistance to intergranular shear. Removal of contacts between grains must precede shear and, since it could lead to the reappearance of contacts between areas of less highly stressed surface and, hence, maintenance of the microstructure, stress induced dissolution is a plausible mechanism for this.

The resistance to plastic deformation is greater in compression than in tension (compare Figs. 3 and 4 with Figs. 7 and 9). The greater strength in compression is attributed to elastic deformation of grains compacted parallel to the direction of compression. At large compressive stresses, the nominal stress versus crosshead displacement relationship is observed to depart from linearity, see Fig. 7, and the subsequent deformation is accompanied by the development of internal cavities, examples of which are shown in Fig. 10. The fact that the cavities are located at the boundaries between adjacent crystalline regions indicates that the mode of deformation is intergranular shear. The stress corresponding to the departure from linearity is a function of both temperature and strain-rate, and application of rate theory yields an activation energy of $\sim$200 kcal mol^{-1}.

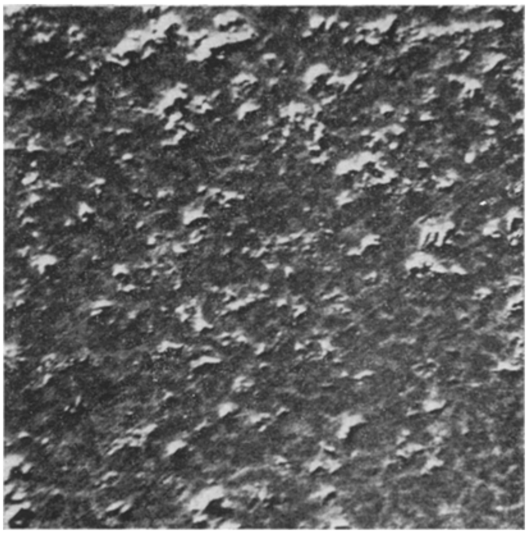

Figure 10 Cavities in polished section of a specimen deformed past the maximum compressive stress (×1000).

The maximum compressive stress and subsequent "work-softening" is interesting since it suggests the possibility of hot forming glass-ceramics. Apart from grain-boundary cavitation, the microstructure is indistinguishable from that in the as-cast condition. Some insight into the

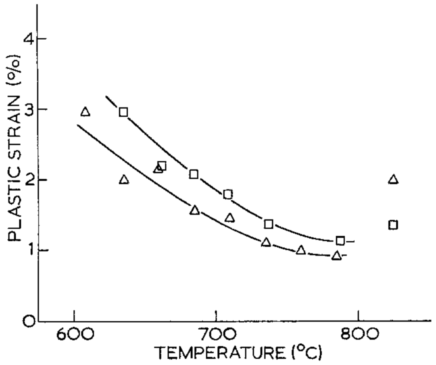

Figure 11 Strain-rate variation of the plastic strain corresponding to the maximum compressive stress. Nominal strain-rates, △, 3×10^{-4} sec^{-1}, □, 3×10^{-3} sec^{-1}.

softening phenomenon can, however, be gleaned from the observation that, for a given temperature, the plastic strain to maximum stress increases with increasing strain-rate, Fig. 11. This suggests that the maximum stress is associated with the thermally activated break-down of a strain-hardening mechanism.

References

1. R. MORRELL and K. H. G. ASHBEE, *J. Mater. Sci.* **8** (1973) 1253.
2. P. W. MCMILLAN, "Glass-Ceramics" (Academic Press, London, 1964) pp. 134-43.
3. *Idem*, private communication (1965).
4. V. N. FILIPOVICH, The structure of glass in "Structural Transformations in Glasses at High Temperatures", Vol. 5 (edited by N. A. Toropov and E. A. Porai-Koshits) (Consultants Bureau, New York, 1965) pp. 23-33.
5. G. W. MOREY, "Properties of Glass". Amer. Chem. Soc. Monograph (1938)
6. J. E. STANWORTH, "Physical Properties of Glass" (Oxford Univ. Press, 1950).
7. K. H. G. ASHBEE, R. LYALL and D. WHITE, *Phil. Mag.* **17** (1968) 225.

Received 21 August and accepted 21 September 1973.